Evolutionary Algorithm Based On Soft Computing Techniques Used in Forward Converter for Sustainable Applications and Energy Factor Approach

Alagu Dheeraj, *Member, IEEE, alagudheeraj@ssn.edu.in* and

V. Rajini, *Senior Member, IEEE, rajiniv@ssn.edu.in*

***Abstract*—Many sophisticated ac/dc or dc/ac converters with varied degrees of complexities are available for low voltage, high current applications like photovoltaic cells, fuel cells, hybrid electric vehicles, telecommunication power supplies and battery chargers., In dc-dc, converters like buck, boost, buck-boost are widely used. In this paper, the mathematical modeling based on various energy parameters like stored energy, pumped energy, and time constant, damping constant is done and analysis are carried out on isolated forward converter with self- driven synchronous rectifier with current double rectifier. The isolated forward converter suits the requirements of the above said applications. Also, the performance of the converter is analyzed with a controller whose parameters are selected using conventional tuning method and soft computing approach like particle swarm and whale optimization techniques.**

***Index Terms*—Active Clamp, Forward Converter, Current Double Rectifier, Energy Factor and DC-DC Modeling, PI controller, Particle Swarm Optimization algorithm, Self-Driven Synchronous Rectifier, Whale Optimization Algorithm.**

I. INTRODUCTION

High power density DC-DC converters make the electronic systems of various industrial space flight systems smaller, lighter and more efficient [1], [2]. The efficiency of these converters is the key factor influencing the power density. The heat/power losses tend to reduce the life and reliability of these converters. The transfer function and state space analysis are used in design and analysis of mathematical modelling for fundamental converters. Transfer function approach of system modeling provides final relation between output variable and input variable. However, a system may have other internal variables of importance and state variable representation considers all such internal variables. Moreover, controller design using classical methods, e.g., root locus or frequency domain method are limited to only LTI systems, particularly SISO (single input single output) systems; since for MIMO (multi input multi output) systems controller design using classical approach becomes more complex. These limitations of classical approach led to the development of state variable approach of system modeling and control which forms a basis of modern control theory. State variable models are basically time domain models, where the dynamics of some variables called state variables which along with the input represent the state of a system at a given time are taken into consideration. These models will automatically adjust to any shift in parameters. State space representation is best suited for both theoretical solutions like analytical and optimization, and numerical calculations.

As the complexity of the circuit increase, so does the order of differential equation which leads to difficulty in time domain analysis. Power DC-DC converters consists of DC power supply source, pump-circuit to transfer energy from supply to passive energy storage elements, filter circuit with passive elements like inductors, capacitors and load. Load could be resistive, back EMF or battery. Energy Factor parameters [18] like pumped energy, stored energy, energy loss, etc., which give the relation between time domain response of dc-dc converter and all the energy storage devices in a switching period are derived. A dc-dc converter is an energy storing device as it has energy storing components like inductors and capacitors. When the converter performance changes from one steady state to another, the stored energy also changes. The inductor currents and capacitor voltages varies in the process of conversion. This variation results in oscillation of the stored energy of the inductors and capacitors. These oscillations of total stored energy determine the boundary condition between continuous conduction mode (CCM) and discontinuous conduction mode (DCM) operations. These parameters are useful in design and analysis of the converter. Energy Factor for various conventional non-isolated converters like Buck, Boost, Super-lift converter have been done by F.L. Luo [18], [23], [24]. However, literature is sparse for similar work on isolated converters. This mathematical modeling for isolated forward converter is described in this paper.

Ms. Alagu Dheeraj, Assistant Professor is with Electrical and Electronics Engineering Department, SSN College of Engineering, Anna University, Chennai 603 110, India (e-mail: alagudheeraj@ssn.edu.in).

Dr. V. Rajini, Professor is with Electrical and Electronics Engineering Department, SSN College of Engineering, Anna University, Chennai 603 110, India (e-mail: rajiniv@ssn.edu.in).

This paper provides a complete analysis and mathematical model of Active Clamp Forward converter [8] with CDR using SDSR [9] - [14], [15], [16], [17] using the energy factor approach as suggested by Luo [18]. The constrained Ziegler Nichols PI controller response is compared with optimizing techniques such as particle swarm optimization (PSO) and whale optimization algorithm (WOA).

The performance of forward converter [19] mainly depends on core resetting technique. The magnetic energy of the core is recycled which would otherwise result in the current build up at each switching cycle saturating the core. Active clamp reset [20], [21] has better performance than other resetting methods like RCD, two switch forward converters, tertiary winding etc., and it overcomes 50% duty cycle limitation with minimal component stress. There are other standard techniques available to operate forward converter above 50% duty cycle such as

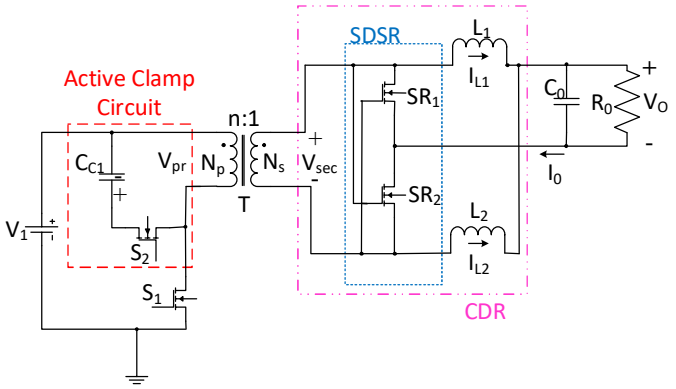

Fig 1: Circuit diagram for active clamp forward converter with SDSR and CDR

introducing tertiary winding. It must withstand twice the input voltage but cause very high switching stresses. In RCD clamp, the cost less than tertiary winding. The design is complicated. and dissipates energy. Finally, 2-switch forward converter is easy to implement. But limits the stress to input voltage switch and diodes with complicated driving circuit.

The transformer core is better utilized in the active-clamp reset method [22]. This is due to the transformer core being energized in both the halves of the switching cycle. This method is a better solution for improving the functioning of the forward converter.

By choosing the appropriate leakage inductance and precise gate turn on/off the switches, noise and ringing could be avoided. Conventional Active Clamp Forward Converter (ACFC) is limited 50% duty cycle operation. By increasing turns ration duty cycle is stretched beyond 50%. Thereby primary side conduction losses are reduced. A low forward voltage drop switch can be selected. Hence lower breakdown rating of rectifier on secondary side. The efficiency of the secondary side of the converter can further be improved by Current Double Rectifier (CDR) with half bridge, full bridge, push-pull or forward converter [3], [4]. ZVS operation of synchronous rectification without additional driver circuit for high current applications reduces conduction losses [5], [6]. Further CDR [7] reduces the current ripple, and the required output capacitor rating. The degree of ripple cancellation is dependent on duty cycle. The use of two output inductors each carrying half the total current (at half the switching frequency), helps is distributing the heat losses significantly which is the important factor in high current designs. In this paper, case study on Active Clamp Forward Converter with SDSR based CDR is done.

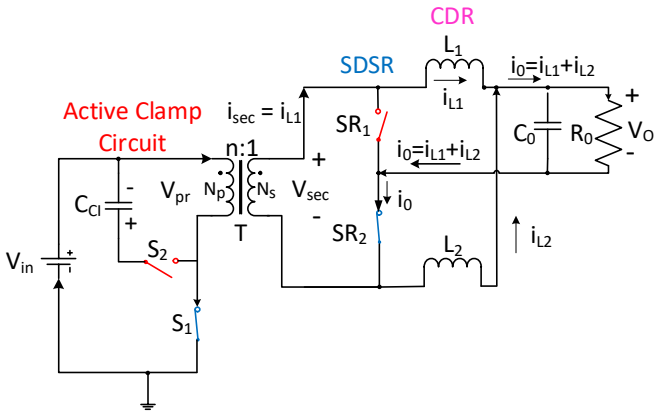

Fig 2a : Mode I

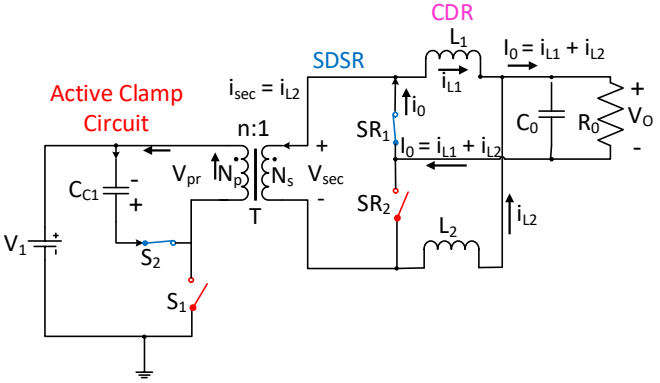

Fig 2b : Mode II

II. ACTIVE CLAMP FORWARD CONVERTER

A. Principle of operation

An active clamp forward converter with self-driven synchronous rectifier based current double rectifier (as shown in Fig.1) is taken for case study. The circuit consists of main switch S_1, active clamp comprising of auxiliary switch S_2 and clamping capacitor C_{cl}, on primary side. The output inductors L_1, L_2, SR_1 and SR_2 at the secondary side of the transformer forms Current Double Rectifier Circuit (CDR). The converter energy is transferred during on time of main switch S_1 and C_{cl} is charged through body diode of S_2. During off time of S_1, energy of parasitic capacitance of S_1 and leakage magnetizing inductance L_m of transformer are discharged through clamping capacitor C_{cl}. Capacitor C_{cl} resets flux of transformer core and zero voltage switching to turn on the switch.

At the secondary of the transformer, load is connected through CDR circuit. In high current applications, with low output voltage results in large power dissipation. By having

CDR at the output, the load current is shared between the two inductors and reduces heat dissipation and conduction losses.

B. Modes of Operation

It consists of active energy transfer, core resetting and freewheeling stages. The ACFC-SDSR consists of two modes. Fig.2. a. shows Mode I: Main switches S_1 and SR_2 on, S_2 and SR_1 off.: where the active energy is transferred from source to load. Fig.2.b. shows Mode II operation. Auxiliary switch S_2 and SR_1 on, S_1 and SR_2 off, where core resetting takes place. Key waveforms of the converters are shown in Fig.2.c. The detailed operation is described below.

There are five stages during a switching cycle.

Stage 1[t0-t1]: The main switch S_1 is turned on at t = t0. Simultaneously gating pulse from transformer secondary side turns on SR_2. The output current i_0 flows through inductor L_2, C_0 and R_0; there by inducing primary current of the transformer. The magnetizing inductor L_m is charged linearly by input voltage V_{in}.

The output current i_0 flowing through CDR inductors, charges the inductor L_2 and discharges the inductor L_1. This stage ends at t = t1, when the main switch S_1 and SR_2 are turned off while SR_1 is turned on.

Stage 2[t1-t2]: After the main switch S_1 is turned off at t1, the clamping capacitor C_{cl} is charged by the reflected load current in the primary winding, i_0/n. This stage ends when V_{S1} reaches the input voltage V_{in} at t2.

Stage 3[t2-t3]: After V_{S1} reaches Vin, the secondary voltage becomes zero and the transformer is shorted. Since the rectifier current cannot to reduce to zero immediately, it starts to resonate. It continues to resonate until $V_{cl} = V_{in} + V_{cl}$. The output current i_0 lowing through CDR inductors, discharges the inductors L1 and L2. This stage ends at t = t3.

Stage 4[t3-t4]: At t = t3, core resetting stars by turning on auxiliary switch S_2 by ZVS. At t = t4, when the clamping capacitor current reaches zero it starts discharging. Current flowing through inductor L_2 continues to decrease whereas inductor current L_1 increases.

Stage 5[t4-t5]: During this interval clamping capacitor discharges completely. The magnetizing current flows in the opposite direction through S_2. At t = t5, S_2 is turned off. This stage ends at t = t5.

At all-time the load current is shared between the two inductor currents i.e., $i_0 = i_{L1} + i_{L2}$.

Fig. 2.c. shows various key waveforms of ACFC. Where V_{s1} and V_{s2} are main and auxiliary switch voltages; I_m – magnetizing current; I_{cl} clamping capacitor current; SR_1 and SR_2 – SRs gating pulses and CDR – I_{L1} and I_{L2} output filter inductor currents.

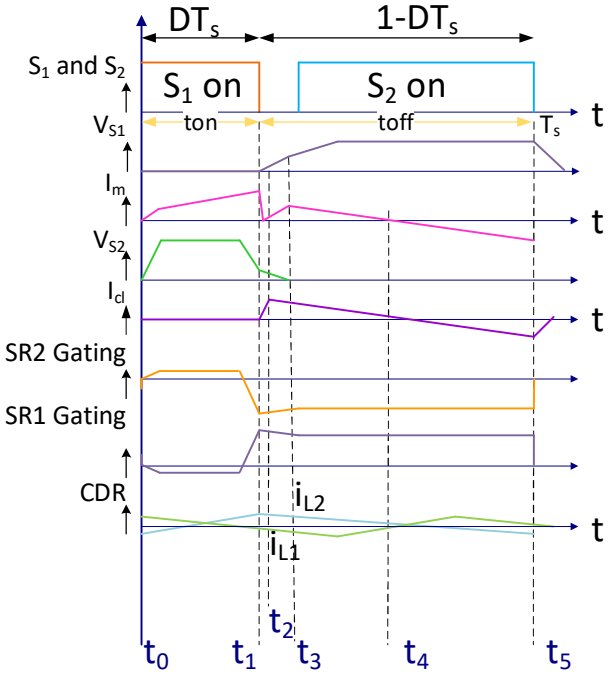

Fig 2c : Key wave forms of the ACFC converter

III. SELECTION OF COMPONENTS

The forward converter is designed for 2.5V / 15A / 100 kHz applications. The input voltage range of 150 ~ 250 V and duty cycle range of 0.36 to 0.63 were assumed. Table I. gives the design specifications and component selection.

The basic design equations of active clamp forward converter are used in selecting the components.

Turns ratio, $$n = \frac{V_{in(\min)} V_{in(\max)}}{V_0 (V_{in(\min)} + V_{in(\max)})} \quad (1)$$

Clamping Capacitor, $$C_c = \frac{\Delta i_m (1 - D_{\min})^2}{1.6 * V_{DC(\max)} * f_{sw}} \quad (2)$$

Resonant frequency, $$f_0 = \frac{(1 - D_{\max})}{2\pi \sqrt{L_m C_c}} \quad (3)$$

Output filter inductor, $$L_0 \geq \frac{V_0 (1 - D_{\min})}{(\Delta i_0)_{ripp} * f_{sw}} \quad (4)$$

Where $L_1 = L_2 = 2L_0$

As each inductor value of the CDRs is twice that of output filter inductor.

Output capacitor, $$C_0 = \frac{(\Delta I_0)_{ripp}}{8 * f_{sw} * (V_0)_{ripp}} \quad (5)$$

$(\Delta I_0)_{ripp}$ 10% of I_0 and $V_{0(ripp)}$ 0.1% of V_0, where $(\Delta I_0)_{ripp} = (\Delta I_{sec})_{max}$

TABLE 1
DESIGN PARAMETERS AND COMPONENTS

Parameters/Components	Value
Maximum Power (P0)	50 W
Input Voltage (Vin)	200 VDC
Output Voltage (V0)	2.5 V
Output Current (I0)	15 A
Switching Frequency(fsw)	100 kHz
Transformer turns ratio (n)	12
Clamping Capacitor (Ccl)	40 nF
CDR Inductors (L1 & L2))	30µH each
Output Capacitor (C0)	660 µF
Load Resistor(R0)	0.165Ω

A. Controller optimization

. The closed loop response of PI controller is analyzed with the conventional Ziegler Nichols method. To further improve the performance, soft computing algorithms such as PSO and WOA are used with an objective function of minimizing the steady state error. Using Ziegler Nichols algorithm [25], the estimated set value for PI controller parameters such as K_p and K_i were determined. Using these values as guide line, optimization is done with PSO [26] and WOA [27] methods. PSO is a global optimization method which depends on few parameters, whereas WOA is a multi-threshold method used to improve the accuracy. The optimal value is obtained based on minimal steady state error.

With the set output voltage of 2.5V, the response of the controller using the parameters obtained from the two optimization algorithms are compared with the conventional Ziegler – Nichols method and the results are given in Table II. Fig.3 shows the closed response of ACFC for Z-N, PSO and WOA methods.

TABLE 1I
CONTROLLER PARAMETERS

	Z-N	**PSO**	**WOA**
K_p	1.3	1.283	***1.2***
K_i	500	429	***494***
$t_{s(ms)}$	6	5	***4***
M_p(%)	48	36	***32***

where K_p-proportional gain, K_i-integral gain, t_s-settling time and M_p-percentage overshoot

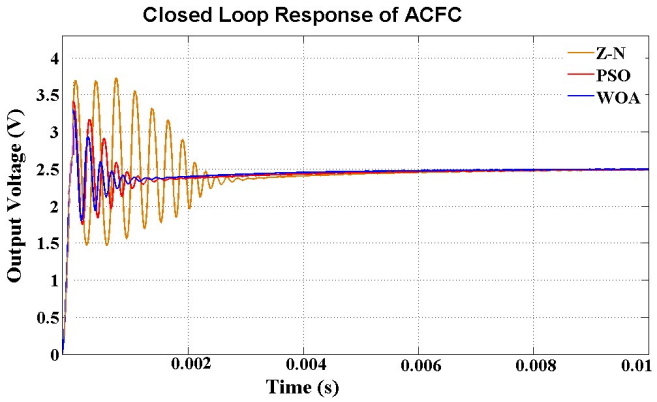

The percentage peak overshoot for Z-N, PSO and WOA are 48, 36 and 32 respectively. In Z-N method the overshoot period is

Fig.3. Closed Loop response of ACFC for Z-N, PSO and WOA methods (V0 Vs T)

greater and gives an under damped response. The PSO gives moderate response. The WOA method gives better closed response with minimal overshoot of 32% and fast settling time of 4ms. The steady state error for all the above methods was zero.

IV. SIMULATION RESULTS AND DISCUSSION

Simulation of the Active Clamp Forward Converter with SDSR is done in MATLAB. Gating pulse for main switch S_1 along with auxiliary switch S_2 and transformer peak value of primary 200V and secondary 5V. Active clamp circuit gives a voltage of 100V and current of 1A. Fig.3. a. shows the waveforms for CDR inductors currents (I_{L1} & I_{L2}) and

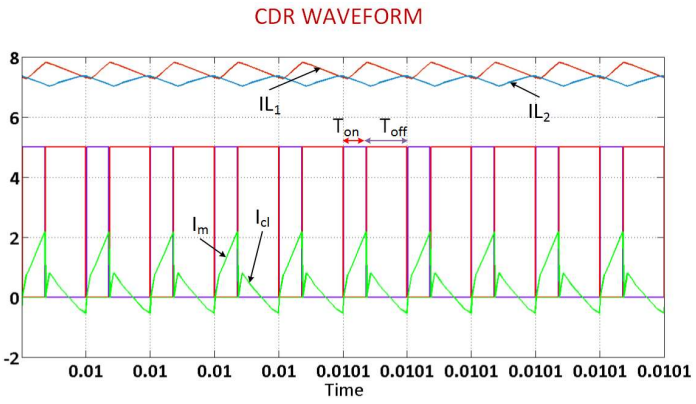

Fig.3.a. CDR output inductor currents and magnetizing current I_m

magnetizing current I_m. The output current of 15A is shared between the two inductors. It is observed that the two inductor currents are asymmetric and the simulated average currents are close to the calculated results. During core resetting period when the active clamp circuit is turned ON, the clamping capacitor is charged during that time. Turning on of S_1 and S_2 by Zero Voltage Switching (ZVS) i.e., when the V_{ds} of corresponding switches reaches zero current increase. Similarly turning on of Synchronous switches SR_1 and SR_2 by ZVS.

The Converter output voltage of 2.5Vand current of 15A is shown in Fig.4.

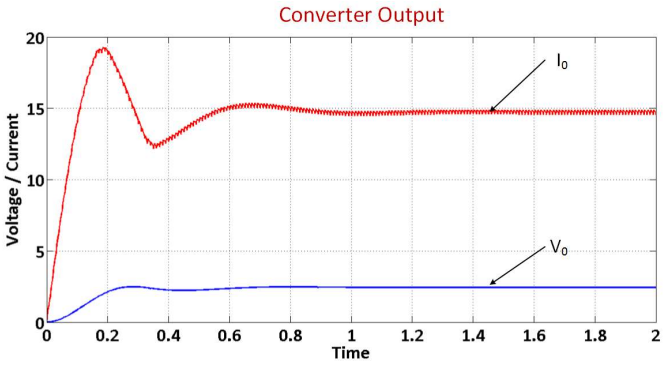

Fig.4. Output voltage and current waveforms

V. MATHEMATICAL MODELING FOR POWER DC-DC CONVERTERS

Traditional mathematical modelling of power converter are done by various experts and the Mathematical modelling for all power DC-DC converter is given as,

$$G(s) = \frac{M}{(1 + s\tau + s^2\,\tau\tau_d)} \tag{6}$$

Where G(s) – transfer function; M – voltage transfer gain; τ – time constant; τ_d – damping constant; s – Laplace Transform in s-domain

From Mode I of Fig.2.a. , input impedance is given as,

$$z_{in}(s) = \frac{V_{in}}{n} + sL_1 + R_0 \| C_0 \| sL_2 \tag{7}$$

expanding eqn. (7), we get

$$= \frac{\left[\frac{V_{in}}{n}\left(s^4 L_2 R_0 C_0 + sL_2 + R_0\right) + s^3 L_1 L_2 R_0 C_0 + s^2 L_1 L_2 + sR_0(L_1 + L_2)\right]}{(s^2 L_2 R_0 C_0 + sL_2 + R_0)} \tag{7a}$$

From Mode II of Fig.2.b., input impedance is given as,

$$z_{in}(s) = \frac{V_{in}}{n} + sL_2 + R_0 \| C_0 \| sL_1 \tag{7b}$$

Solving eqn. (7b), we get

$$= \frac{\left[\frac{V_{in}}{n}\left(s^4 L_1 R_0 C_0 + sL_1 + R_0\right) + s^3 L_1 L_2 R_0 C_0 + s^2 L_1 L_2 + sR_0(L_1 + L_2)\right]}{(s^2 L_1 R_0 C_0 + sL_1 + R_0)} \tag{7c}$$

Also,

$$\frac{V_0}{V_{in}} = \frac{R_0 \| C_0}{L_1 + (R_0 \| C_0)} \tag{8}$$

Solving eqn. (8), we get

$$= \frac{R_0}{(sR_0C_0 + 1)} \tag{8a}$$

Since Mode I and Mode II are symmetric, the transfer function G(s) for the ACFC converter is determined using equation (7a) or (7c) by state space analysis. G(sL) in terms of components listed from Table1 is given as

Using eqn. 7a. and 8a., transfer function G(s) is obtained as,

$$G(s) = \frac{M.R_0}{(sR_0C_0 + 1)} \cdot \frac{(s^2 L_2 R_0 C_0 + sL_2 + R_0)}{\left[\frac{V_{in}}{n}\left(s^4 L_2 R_0 C_0 + sL_2 + R_0\right) + s^3 L_1 L_2 R_0 C_0 + s^2 L_1 L_2 + sR_0(L_1 + L_2)\right]} \tag{9}$$

-

TABLE III
ENERGY FACTOR PARAMETERS

Energy Factor Parameters	Symbol & Formulae	Values
Pumped Energy	$PE = V_1 I_1 T$	6 *(mJ)*
Stored Energy	$SE = \sum_{j=1}^{n_L} W_{Lj} + \sum_{j=1}^{n_c} W_{Cj}$	88.93 *(mJ)*
Energy Loss	$EL = \int_0^T P_{loss}\,dt = P_{loss}\,t$	0.6 *(mJ)*
Output Energy	$P_0 = (PE - EL)T$	5.4 *(mJ)*
Efficiency	$\%\eta = \frac{P_0}{P_{in}} = \frac{PE - EL}{PE}$	90%
Capacitor to Inductor Ratio	$CIR = \frac{\sum_{j=1}^{n_C} W_{C_j}}{\sum_{j=1}^{n_L} W_{L_j}}$	8.2663
Time Constant	$\tau = \frac{2T.EF}{1 + CIR}\left[1 + CIR\left(\frac{1-\eta}{\eta}\right)\right]$	5.374 *(μs)*
Damping Time Constant	$\tau_d = \left[\frac{2T.EF}{1 + CIR}\right].\left[\frac{CIR}{\eta + CIR(1-\eta)}\right]$	13.412 *(μs)*
Time Constant ratio	$\xi = \frac{\tau_d}{\tau} = \frac{CIR}{\eta\left[1 + CIR\left(\frac{1-\eta}{\eta}\right)\right]^2}$	2.494

Neglecting L_2 and higher order terms, and rearranging eqn. (9) we get,

$$G(s) = \frac{M.R_0.\frac{n}{V_{in}}}{\left[s^2 C_0 L_1.\frac{n}{V_{in}} + s\left(R_0 C_0 + L_1 \frac{n}{V_{in}}\right) + 1\right]} \quad (10)$$

Where Eqn. 10 is of the general form of eqn. 6.

$$\tau = R_0 C_0 + L_1 \frac{n}{V_{in}} \quad (10a)$$

$$\tau\tau_d = C_0 L_1 . \frac{n}{V_{in}} \quad (10b)$$

Substituting eqn. 10a. in eqn. 10b. we get τ_d as,

$$\tau_d = \frac{R_0 C_0 L_1 n}{\left(R_0 C_0 V_{in} + n L_1\right)} \quad (10c)$$

VI. Energy Factor

For the ACFC shown in fig.1.energy factor and its parameters are determined. The input energy of the source is pumped into the circuit and the energy is distributed to all the energy storing devices like inductors and capacitors. The following equations give the relationship between transfer function and stored energy in power DC-DC converters [18]. The SDSR converter is analyzed in terms of, PE - Pumped Energy, SE - Stored Energy, EL - Energy Losses, η - Efficiency, CIR - Capacitor to Inductor Ratio, τ – Time constant and τ_d – damping constant.

The input energy in a switching period T is given as Pumped Energy(PE). Total energy stored in inductors and capacitors are represented SE. The ACFC shown in fig .1 has Vin as PE, C_{cl}, C_0, L_1 and L_2 are the energy storing elements SE.

Energy stored in inductor (W_L) and capacitor (W_c) are,

$$W_L = \frac{1}{2} L I_L^{\,2}; W_c = \frac{1}{2} C V_c^{\,2} \quad (11)$$

and the total energy stored in inductor due to L_1 and L_2 is given as,

$$W_L = W_{L1} + W_{L2} \quad (12)$$

The total energy stored in Clamping capacitor(C_{cl}) and output capacitor(C_0) is,

$$W_c = W_{cl} + W_{c0} \quad (13)$$

Power loss during conversion process due to resistance, leakage inductors and parasitic capacitor and power losses in semiconductor switching devices is given as Energy loss (EL),

$$EL = \int_0^T P_{loss} dt = P_{loss} t, \text{ where } P_{loss} = P_r + P_e + P_d \quad (14)$$

Where P_r – resistive power loss, P_e – passive element power loss and P_d – device power loss

Output power (P_0) = $V_0 I_0$ and Input power (P_{in}) =P_0+P_{loss} (15)

Output energy in period T, $P_0 = (PE - EL)T$ (16)

For the ACFC with SDSR, transfer function G(s), and gain(M) from (10) is given as,

$$G(s) = \frac{0.0165}{72.0841 s^2 + 5.374 s + 1} \text{ and}$$

$$M = \frac{V_2}{V_1} = 0.0165$$

Using formulae of the Energy Factor parameters like PE, SE, τ, τ_d, ξ, σ, and ω, were calculated at various converter efficiencies. Table III. shows the energy factor parameters at 90%. Since time constant ratio(ξ) > 0.25, output wave form is oscillatory and over shoot occurs. System performance can be further improved by PI controller

Parameters	Efficiency (η)		
	70%	80%	90%
Time Constant (τ) μs	12.726	8.591	5.375
Damping Constant (τd) μs	7.2826	9.4397	13.412
Time Constant Ratio (ξ)	0.572	1.0988	2.495
Damping Factor (σ)Hz	68656.8	52967.78	37280.05
Frequency(ω)	96157.83	97598.196	111723.098

.

TABLE IV
ACFC ENERGY FACTOR PARAMETERS PERFORMANCE AT VARIOUS EFFICIENCIES

Step input response for the converter is

$$g(t) = V_2\left[1 - e^{-t/2\tau_d}\left\{\left(\cos\omega t\right) - \frac{1}{\sqrt{\frac{4\tau_d}{\tau} - 1}}\left(\sin\omega t\right)\right\}\right] \quad (17)$$

where V_2 is the output voltage.

Table IV. shows the energy factor parameters for three different efficiencies viz. 70%, 80% and 90%. Since time constant ratio(ξ) > 0.25, output wave form is oscillatory and over shoot occurs. 70% efficiency converter give better performance. With PI controller, system performance with higher efficiencies can be achieved.

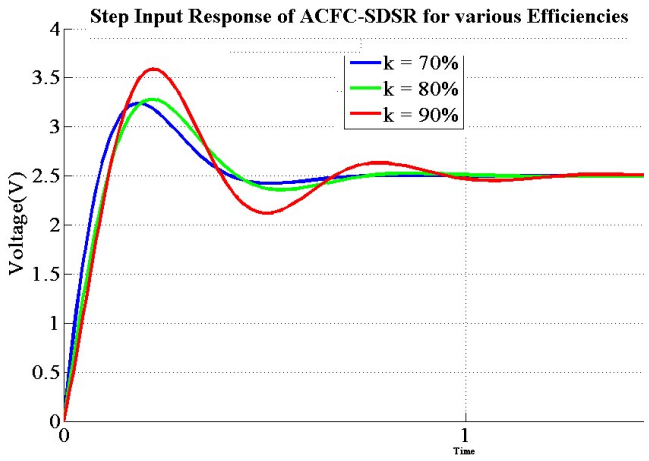

Fig.5 : Output voltages for various efficiencies using energy factor

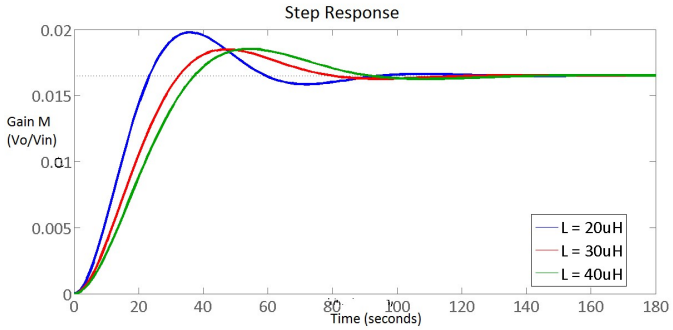

Fig.6: Converter response for various inductors, M Vs t

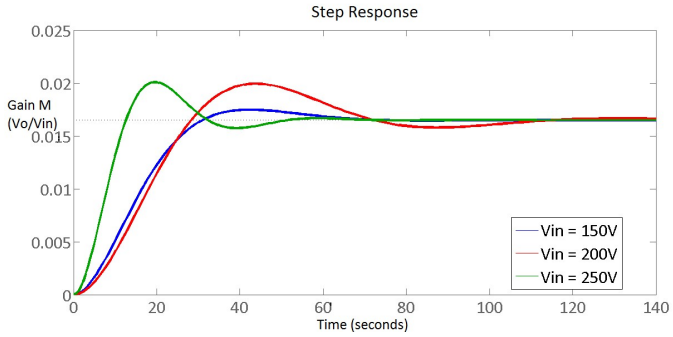

Fig.7: Converter response for various input voltage, M Vs t

Fig. 6. Shows the simulated time response for various inductor (L_1 and L_2) values at a constant input voltage of V_{in} = 200V. It is noticed that, converter performance is better at 30µH inductor value. Time response of various input voltage ranging 150~250V with inductors L_1 and L_2 , 30µH each is shown in Fig. 7. It is observed that, with input voltage, Vin = 200V the converter gives better response. Simulated results show that the DC model and analysis are the same in Section III.

VII. CONCLUSION

For high current applications, Active Clamp Forward Converter with CDR using SDSR is analyzed with energy factor parameters in this paper. Compared to half bridge or full bridge converter on front end, the active clamp forward converter using SDSR with CDR improves overall efficiency with high power density. A novel method of the time domain analysis for the isolated converter is done based on the energy factor parameters. For any values and any number of stored energy components like capacitors and inductors, the system performance can be determined in terms of its energy. This throws light on the performance of energy devices in a converter and their response. Compared to conventional methods this energy factor approach gives better understanding of energy storing elements. Also, the closed loop control of the converter is done using PI controller using various optimization algorithms and WOA is found to offer a better transient and steady state performance while the other methods such as PSO and Z-N offered a good steady state performance alone

REFERENCES

[1] Kudo T, Toi T, Kaneko Y, Abe S, “Contactless Power Transfer System Suitable For Low Voltage and Large Current Charging For EDLCs”, in International Power Electronics Conference (IPEC-Hiroshima 2014 - ECCE-ASIA) pp.1109 – 1114, 2014

[2] Marzouk, M, Ferrieux J P,Frey D, Sarrazin B, “A shared traction drive and battery charger modes for Plug-In Hybrid Electric Vehicle application”, in 16th European Conference on Power Electronics and Applications (EPE’14-ECCE-Europe), pp.1-10, 2014

[3] Ke Jin, Zhijun Liu, Xiaoyang Yu, Xiaoyong Ren, “A Self-Driven Current-Doubler-Rectifier Three-Level Converter With Integrated Magnetics”, in IEEE Trans. Power Electronics Vol.29, pp.3604 – 3615, 2014

[4] Pan Xuewei, Rathore A K, “Naturally Clamped Zero-Current Commutated Soft-Switching Current-Fed Push–Pull DC/DC Converter: Analysis, Design, and Experimental Results”, in IEEE Trans. Power Electronics Vol.30, pp.1318 – 1327, 2015

[5] Sung-Sae Lee, Seong-Wook Choi, Gun-Woo Moon. (2007). High-Efficiency Active-Clamp Forward Converter with Transient Current Build-Up (TCB) ZVS Technique. IEEE Trans. Ind. Electronics 54, pp.310 – 318.

[6] Chen Shin-Ju, Huang Chao-Ming, Yang Sung-Pei, Sheng-Hsiang Chiang, “An Interleaved ZVS Forward Converter with Series Input Parallel Output Structure”, in 9th IEEE Conference on Industrial Electronics and Applications (ICIEA), pp.379 – 384, 2014

[7] Lee Jong-Jae, Bong-Hwan Kwon. (2007). DC–DC Converter Using a Multiple-Coupled Inductor for Low Output Voltages. *IEEE Trans. Ind. Electronics 54,* pp. 467 – 478

[8] Shijia Yang, Zhaoming Qian, Qian Ouyang, Peng, F.Z. “As improved Active Clamp Forward Converter”, in 23rd IEEE Annual Applied Power Electronics Conference and Exposition, APEC 2008, pp.318 – 322, 2008

[9] Ting Qian, Wei Song, Lehman B,”Self-Driven Synchronous Rectification Scheme Without Undesired Gate-Voltage Discharge for DC-DC Converters With Symmetrically Driven Transformers”, in IEEE Trans. Power Electronics Vol.23, pp.506 – 510, 2008

[10] Fernandez A, Lamar D.G., Rodriguez, M., Hernando M.M., Sebastian, J., Arias M,” Self-Driven Synchronous Rectification System With Input Voltage Tracking for Converters With a Symmetrically Driven

Transformer", in IEEE Trans. Ind. Electronics Vol.56, pp.1440 – 1445, 2009

[11] Ke Jin, Ming Xu ,Yi Sun, Sterk, D Lee, F C, "Evaluation of Self-Driven Schemes for a 12-V Self-Driven Voltage Regulator", in IEEE Trans. Power Electronics,Vol.24, pp.231-2322 ,2009

[12] Zhong, W X Zhong, W P Ho, W C Hui S Y, "Generalized Self-Driven AC–DC Synchronous Rectification Techniques for Single- and Multiphase Systems", in IEEE Trans. Ind. Electronics Vol.58, pp.3287 – 3297, 2011

[13] Zhong, W X, Hui, S Y Ho, W C Xun Liu,"Using Self-Driven AC–DC Synchronous Rectifier as a Direct Replacement for Traditional Power Diode Rectifier", in IEEE Trans. Ind. Electronics Vol.59, pp.392 – 401, 2012

[14] Junming Zhang, Jiawen Liao, Jianfeng Wang, Zhaoming Qian, "A Current-Driving Synchronous Rectifier for an LLC Resonant Converter with Voltage-Doubler Rectifier Structure", in IEEE Trans. Power Electronics Vol.27, pp.1894 – 1904, 2012

[15] Xing Xue, Weikang Chen, Baoqiang Li, "The Design Of LED Driving Power Based On Current-Double Synchronous Rectifier ZVZVS", 13th International Conference on Electronic Packaging Technology and High Density Packaging (ICEPT-HDP), pp.1508 - 1511

[16] Bor-Ren Lin, Shih-Kai Chung, Tung-Yuan Shiau, "Zero-Voltage-Switching DC/DC Converter With Three Three-level Pulse-width Modulation Circuit Cells", in IET Power Electronics Vol.6, pp.1-8, 2013

[17] Jae-Won Yang, Hyun-Lark Do, "High-Efficiency ZVS AC-DC LED Driver Using a Self-Driven Synchronous Rectifier", in IEEE Transactions on Circuits and Systems I: Regular Papers Vol.61, pp.2505–2512,2014

[18] Fang Lin Luo, "Analysis of Energy Factor and Mathematical Modeling For Power DC-DC Converters", in HAIT Journal of Science and Engineering, vol. 2, issue 3-4, pp.496 – 528, 2005

[19] Li, Q., Lee, F.C., Jovanovic, M.M., "Design consideration of transformer DC Bias of forward converter with active clamp", in 14th Annual Applied Power Electronics Conference and Exposition,. APEC '99, vol. 1, pp.553-559, 1999

[20] Byoung-Hee Lee, Young-Do Kim, Moon-Young Kim, In-Ho Cho, Gun-Woo Moon,"Active-clamp Forward Converter With Asymmetric Transformer Turns For Reducing Transformer DC Offset Current", IECON 2012 – 38th Annual Conference on IEEE Industrial Electronics Society pp.204 – 209, 2012

[21] Hwu, K I, Yau Y T, "High Step-Up Converter Based on Coupling Inductor and Bootstrap Capacitors With Active Clamping", in IEEE Trans. Power Electronics Vol.29, pp.2655 – 2660, 2014

[22] Gu, B, Dominic J, Chen B, Zhang L, Lai J, "Hybrid Transformer ZVS/ZCS DC–DC Converter With Optimized Magnetics and Improved Power Devices Utilization for Photovoltaic Module Applications", in IEEE Trans. Power Electronics Vol.30, pp.2127 – 2136, 2015

[23] Ahmed Hammoda1, Mohammed Buamud, Mahmoud Nasr, Mohamed Tamasas, "Estimation of Advanced DC/DC Luo Converters Based on Energy Factor and Sub Sequential Parameters ", ENERGYCON 2014, Dubrovnik, Croatia, 2014

[24] Fang Lin Luo, Hong Ye, Member, Small Signal Analysis of Energy Factor and Mathematical Modeling for Power DC–DC Converters ", IEEE Trans. Power Electronics Vol.22, pp.69-79, 2007

[25] Oladimeji Ibrahim, Nor Zaihar Yahaya, Nordin Saad,"Comparative studies of PID controller tuning methods on a DC-DC boost converter", in 6th International Conference on Intelligent and Advanced Systems (ICIAS), pp.1-5, 2016

[26] J. B. L. Fermeiro, J. A. N. Pombo, M. R. A. Calado, S. J. P. S. Mariano, "Evaluation of a particle swarm optimization controller for dc-dc boost converters", in 9th International Conference on Compatibility and Power Electronics (CPE),pp. 179-184, 2015

[27] Hany M. Hasanien,"Whale optimisation algorithm for automatic generation control of interconnected modern power systems including renewable energy sources", in IET Generation, Transmission & Distribution, Vol.12, Issue: 3, pp.607-614, 2018